DISCRETE ELEMENT MODELLING OF MULTI-FRACTURING SOLIDS AND STRUCTURES

D.R.J. Owen and D. Peric and S. Mohammadi

Department of Civil Engineering, University of Wales Swansea, Singleton Park, Swansea SA2 8PP, U.K.

A novel approach, based on the discontinuum concepts of the Discrete Element Method, is presented for fracture and delamination analysis of composites subjected to impact loading. A combined finite/discrete element algorithm is developed for damage analysis of the progressive fracturing and fragmentation behaviour which is observed in composite structures. The algorithm comprises various contact detection and contact interaction schemes to construct an efficient and reliable tool for the modelling of complex post failure phenomena. An anisotropic softening Hoffman failure criterion is adopted for specifying the initiation of a crack. A set of numerical tests is provided to assess the performance of the algorithm.

1 INTRODUCTION

Gradually replacing conventional materials, composite laminates are now widely used in many applications involving dynamic loading such as machinery, pressure vessels, defense structures, vehicles, sport equipment and notably aerospace structures [1]. Although today's aircraft structures are still predominantly constructed from lightweight aluminium alloys, comparison of the proportions of materials used in the design of aircraft structures during the last two decades would indicate an increasing trend towards usage of polymeric based composite materials. It is also widely accepted that there exists a significant future prospect for a substantial increase in the contribution of advanced composite materials to the design of new aircraft. Industries such as the automotive, and recreational industries have also been placing increased reliance on for high performance materials [2].

One of the major problems that affects the design and performance of composite materials for structural applications is their vulnerability to transverse impact which may cause substantial internal damage of the component due to matrix cracking, fibre failure and delamination. By examining the numerous contributions to this area of research [3, 4, 5, 6], it is evident that impact loading of composites represents a highly complex

[3, 4, 5, 6], it is evident that impact loading of composites represents a highly complex phenomenon involving of several interacting processes.

Figure 1 represents the progressive fracturing, delamination and fragmentation phenomena in a typical composite specimen subjected to impact loading. This schematic representation, is perhaps only relevant to the failure observed in high velocity impact. For low velocity impact, extensive fragmentation is unlikely and material fracture and delamination will be the dominant modes of failure.

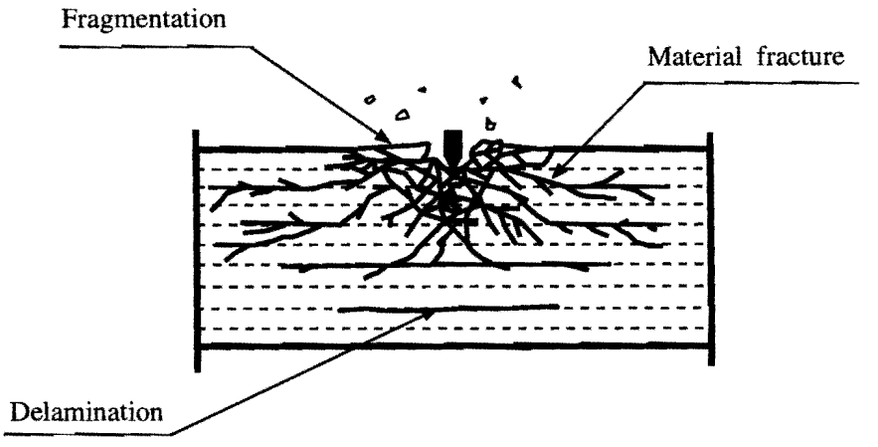

Figure 1: Progressive fracturing, delamination and fragmentation in a typical composite specimen subjected to impact loading.

In general, according to the orthotropic laminated nature of composites, the failure modes may be classified into four different types : matrix failure, delamination, shear cracking, and erosion damage. There is, however, agreement that the most dominant causes of damage during impact are matrix cracking coupled strongly with complex mode delamination mechanisms [7]. These failure modes are accompanied by steep stress gradients and are usually encountered in regions such as free edges, ply termination, zone of delamination, and voids and holes.

The three flexural modes are not always activated in an impact loading of composites. If the projectile has sufficient energy, it may penetrate into the laminate and may cause a large front surface erosion without activating other behaviours [6].

Recent developments of discrete element methods have opened a new approach to modelling this behaviour based on discontinuum mechanics. In contrast, most computational simulations to date have employed continuum based finite elements to evaluate the initiation and propagation of delamination. Similar to other material strength theories, delamination initiation could be basically treated within the theory of plasticity. It is, in fact, a material model for the thin adhesive layer, although it is usually referred to as an out-of-plane property of composite layers.

In early simulations, a simple criterion based on the comparison of normal stress to a maximum cohesion value was used. Later, more complex models were developed for different types of laminates. In the early eighties, continuum elasticity was frequently used to formulate the governing equations for laminate composites [8, 9]. The main

disadvantage of these schemes was their restriction to linear geometry of laminates, and many of them were only formulated for dealing with free edge delaminations [10].

The next step to a more rational model was achieved by development of contact interaction algorithms. Liu *et al* [7] used a contact analysis for modelling the interface behaviour of laminate composites containing multiple delaminations. In a similar scheme, Stavroulakis *et al* [11] employed a contact algorithm and a Coulomb friction law to study the material inclusion problem in composites. In most of these studies, the Chang-Springer delamination failure criterion was used. This model was proposed by Chang and Springer [12] in their work on wooden bends and then was successfully employed in composite applications. Fracture mechanics concepts have been widely adopted in the development of crack propagation algorithms to model the extension of delamination. Several criteria have been proposed to include the effects of individual or mixed modes of fracture [5].

It should be noted that in a real situation, delamination failure is always accompanied by inplane failures, including matrix and fibre fractures. Therefore a comprehensive study of the behaviour of composites subjected to low or high velocity impacts, requires a comprehensive scheme which should be capable of modelling progressive in and out of plane fracturing. The traditional elasticity and fracture mechanics methods are applicable in situations dealing with a low-fractured area. However in a highly fractured region, discontinuum based mechanics has been found to be more appropriate. The treatment of these classes of problems is naturally related to discrete element concepts, in which distinctly separate material regions are considered which may be interacting with other discrete elements through a contact type interaction [13].

In this study, a combined finite/discrete element algorithm is developed to predict initiation, propagation and interaction of fracture and delamination phenomena in composites. In the following, after a general review of the discrete element method, contact interaction formulations will be discussed in detail. Then the crack (material and interlaminar) initiation criteria will be described and certain numerical issues will be addressed. A brief review of crack propagation phenomena will be introduced which includes a discussion on softening behaviour and energy release rate. The ability of the model to correctly simulate this behaviour will be assessed by solving a set of test cases.

2 DISCRETE ELEMENT MODELLING OF COMPOSITE LAMINATES

It has been shown that delamination and material fracture in composites subjected to low or high velocity impact loadings are progressive phenomena which may rapidly propagate throughout the component. This might result in the creation of new totally separated zones, which interact with their surrounding regions. Consequently, a comprehensive scheme is required to monitor the fracturing process and to effectively model both individual and interaction behaviour. Recent developments of discrete element methods have prepared the ground for a new approach to modelling this behaviour based on discontinuum mechanics.

The traditional approach to the simulation of stress distributions in arbitrary shaped components under possible nonlinear geometric and material conditions is by finite element techniques. However, the traditional finite element method (FEM) is rooted in the

concepts of continuum mechanics and is not suited to general fracture propagation problems since it necessitates that discontinuities be propagated along the predefined element boundaries. The corresponding elasticity and fracture mechanics concepts are applicable only in situations dealing with a single crack or a low-fractured area without any fragmentation. In contrast, the discrete element method (DEM) is specifically designed to solve problems that exhibit strong discontinuities in material and geometric behaviour [14]. The *discrete element method* idealizes the whole medium into an assemblage of individual bodies, which in addition to their own deformable response, interact with each other (through a contact type interaction) to perform the same response as the medium. [13]. A far more natural and general approach is offered by a combination of discrete element and finite element methods.

Consider a composite specimen subjected to an impact loading as depicted in Figure 2. Early material cracks and interlaminar debondings are likely to appear near the position of applied impact load. As the analysis advances, two separate regions could be distinguished. The first one is a highly fractured and delaminated region, and the second is the remainder of the body which presumably contains no delamination or fracture patterns. The fractured region is usually formed in the vicinity of the impact loading and may comprise further separate responses.

A computationally efficient elastoplastic analysis can be performed by simple shell or solid elements to determine the individual regions according to some effective stress or strain criteria. The predicted fractured/delaminated regions will then be examined in the later stages of the analysis through the developed combined finite/discrete element algorithm. The interface boundaries will be further extended if either the material fracture or the interlaminar debonding has reached the boundaries of the DEM region.

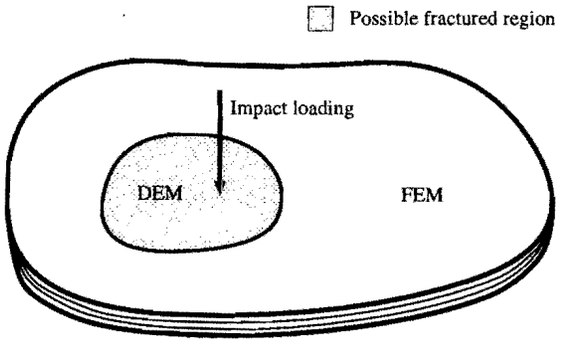

Figure 2: Composite specimen subjected to impact loading.

Figure 3 shows a typical section of the above composite specimen (here, a quarter of a plate). In a combined FE/DE method, the possibly fractured region is modelled using a discrete element mesh and the remainder of the specimen is modelled by a standard finite element mesh. It is also possible to model the whole structure with discrete elements; in which case the possibility of delamination is investigated throughout the structure. A combined mesh enables us to prevent unnecessary contact detection and interaction calculations which comprise a major part of the analysis time. It is worth noting that even by modelling the whole structure with discrete elements, we are still using a combined finite/discrete element approach, owing to the fact that finite elements are used for modelling the deformable behaviour of individual discrete elements.

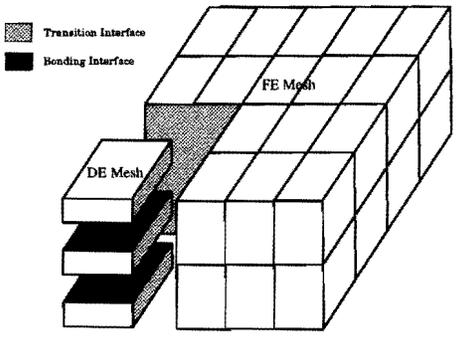

Figure 3: Discrete element modelling of a composite plate.

Each ply or a group of similar plies is modelled by one discrete element. Each discrete element will be discretized by a finite element mesh and may have nonlinear material properties or geometric nonlinearities (large deformations). The interlaminar behaviour of discrete elements is governed by bonding laws, including contact and friction interactions for the post delamination phase.

Interactions between finite elements (not those which are used for DEM discretization) and discrete elements are modelled by transition interfaces. A transition interface is defined as a normal interface with very high bonding strengths which prevent debonding under all loading conditions.

All interfaces, are firstly monitored against the delamination criterion. Once two layers are delaminated, the corresponding interface will still be capable of further contact and friction interaction. However, there will be no re-bonding after delamination.

One important aspect of this type of modelling, which distinguishes it from other contact based delamination algorithms [15, 16], is that it does not require any predefined interface element. Being free from the restrictions of interface elements provides major advantages: Firstly, there is no need for the nodes on different layers to match each other, which eases the way in which data is prepared. This is essential in defining the transition interfaces. Secondly, in progressive cracking, particularly material fracturing, we may end up with new nodes, edges and boundaries that could destroy the compatibility required for these interface elements.

Material fracture may result in the creation of new discrete bodies which are in contact and friction interaction with neighbouring bodies. A special remeshing algorithm is adopted to maintain compatibility conditions in newly fractured regions. Figure 4 represents the two dimensional remeshing algorithm which comprises four steps: splitting the element, separating the failed nodes, creating new remeshing nodes and dividing uncracked elements to enforce compatibility at new nodes. Adopting this local remeshing algorithm will provide a relatively finer mesh in the fractured region which improves the finite element approximation of the analysis. To perform this remeshing technique in three dimensional analysis, further consideration is required. Employing a stabilized pentahedral element, a similar scheme can be adopted for remeshing along the triangular faces of the element, and a simple vertical crack across the thickness of the pentahedral element can effectively model the creation of a new three dimensional crack face.

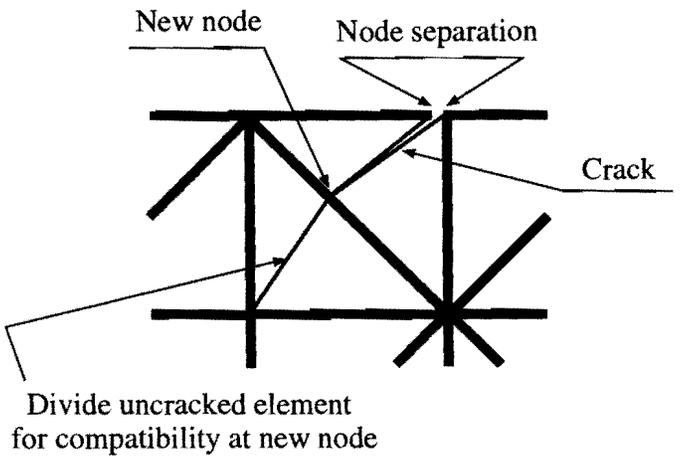

Figure 4: Discrete element fracturing algorithm.

3 EXPLICIT DYNAMIC ANALYSIS

3.1 Governing equations

The standard variational (weak) form of the dynamic initial/boundary value problem is taken as the point of departure. Let Ω represent the body of interest and Γ denote its boundary. In a standard fashion the boundary is assumed to consist of a part with prescribed displacement u_i, Γ_{u_i}, and a part with prescribed traction force f_i^{surf}, Γ_{σ_i}. In addition it is assumed that a part Γ_c may be in contact with another body. By denoting

$$\mathcal{V} := \{\delta \boldsymbol{u} : \delta u_i = 0 \quad \text{on} \quad \Gamma_{u_i}\} \tag{1}$$

as the space of admissible variations, the variational form of the dynamic initial/boundary value problem can be expressed as

$$\mathcal{W}^{\text{int}}(\delta \boldsymbol{u}, \boldsymbol{u}) + \mathcal{M}(\delta \boldsymbol{u}, \boldsymbol{u}) = \mathcal{W}^{\text{ext}}(\delta \boldsymbol{u}) + \mathcal{W}^{\text{con}}(\delta \boldsymbol{u}) \tag{2}$$

where

$$\mathcal{W}^{\text{int}}(\delta \boldsymbol{u}, \boldsymbol{u}) = \int_{\Omega} \delta \boldsymbol{\epsilon}(\boldsymbol{u}) : \boldsymbol{\sigma}(\boldsymbol{u}) dv \tag{3}$$

$$\mathcal{M}(\delta \boldsymbol{u}, \boldsymbol{u}) = \int_{\Omega} \delta \boldsymbol{u} \cdot \rho \ddot{\boldsymbol{u}} dv \tag{4}$$

$$\mathcal{W}^{\text{ext}}(\delta \boldsymbol{u}) = \int_{\Omega} \delta \boldsymbol{u} \cdot \boldsymbol{f}^{\text{body}} dv + \int_{\Gamma_\sigma} \delta \boldsymbol{u} \cdot \boldsymbol{f}^{\text{surf}} da \tag{5}$$

$$\mathcal{W}^{\text{con}}(\delta \boldsymbol{u}) = \int_{\Gamma_c} \delta \mathbf{g}(\boldsymbol{u}) \cdot \boldsymbol{f}^{\text{con}} da \tag{6}$$

denote, respectively, the virtual work of internal forces, the inertial forces contribution, the virtual work of external forces and the virtual work of contact forces. Here $\boldsymbol{\sigma}$ is

the Cauchy stress tensor, ϵ is the strain tensor, $\boldsymbol{u}$ is the displacement vector, while $\mathbf{g}$ represents the contact gap vector. Observe that in the present formulation the contact terms correspond to a penalty formulation of contact interaction.

3.2 FE discretisation and time integration

The standard finite element discretisation of the variational form (2) results in a discrete set of algebraic time dependent equations which may be expressed, in matrix form, as

$$\boldsymbol{M}\ddot{\boldsymbol{u}}(t) + \boldsymbol{f}^{\text{int}}(\boldsymbol{u}, t) = \boldsymbol{f}^{\text{ext}}(t) + \boldsymbol{f}^{\text{con}}(t) \tag{7}$$

where t is the time, $\boldsymbol{f}^{\text{int}}(\boldsymbol{u}, t)$ the internal force vector, $\boldsymbol{f}^{\text{ext}}(t)$ the external force vector, $\boldsymbol{f}^{\text{con}}(t)$ the contact force vector and $\boldsymbol{M}$ denotes the mass matrix.

The velocity $\boldsymbol{v} = \dot{\boldsymbol{u}}$ and acceleration $\ddot{\boldsymbol{u}} = \dot{\boldsymbol{v}}$ are approximated by using the central difference method with variable time steps. Letting a variable with subscript n denote the numerical solution at time station $t = t_n$, we have

$$\boldsymbol{v}_{n+1/2} = \frac{\boldsymbol{u}_{n+1} - \boldsymbol{u}_n}{\Delta t_n} \tag{8}$$

$$\boldsymbol{v}_{n-1/2} = \frac{\boldsymbol{u}_n - \boldsymbol{u}_{n-1}}{\Delta t_{n-1}} \tag{9}$$

$$\boldsymbol{v}_n = \frac{1}{2}(\boldsymbol{v}_{n-1/2} + \boldsymbol{v}_{n+1/2}) \tag{10}$$

$$\dot{\boldsymbol{v}}_n = \frac{\boldsymbol{v}_{n+1/2} - \boldsymbol{v}_{n-1/2}}{\Delta \bar{t}_n} \tag{11}$$

$$\Delta \bar{t}_n = \frac{1}{2}(\Delta t_{n-1} + \Delta t_n) \tag{12}$$

Furthermore, the mass matrix is assumed to be diagonal, so as to avoid solving a set of simultaneous equations at each timestep. Making use of the above approximations, we obtain for the i-th degree of freedom,

$$v_{i,n+1/2} = v_{i,n-1/2} + \Delta \bar{t}_n m_i^{-1} \left((f_i^{\text{ext}})_n + (f_i^{\text{con}})_n - (f_i^{\text{int}})_n \right) \tag{13}$$

where m_i is the i-th diagonal term of $\boldsymbol{M}$. Time incrementation is then readily performed by evaluating displacement, velocity and acceleration using eqns (8), (10) and (11), respectively.

4 CONTACT INTERACTION

Once the possibility of contact between discrete elements is detected (by a contact detection algorithm), contact forces have to be evaluated to define the subsequent motion of the discrete elements from the dynamic equilibrium equation. In a penalty method, penetration of the contactor object is used to establish the contact forces between contacting objects at any given time.

Attention is now focused on a single boundary node in contact to formulate the residual contribution of contact constraint, $\mathbf{r}^c$. The component form of the virtual work of the contact forces associated to the contact node is then given by:

$$\delta W^{\text{con}}(\delta \boldsymbol{u}) = f_k^c \, \delta \mathrm{g}_k = f_k^c \, \frac{\partial \mathrm{g}_k}{\partial u_i^s} \, \delta u_i^s \tag{14}$$

where $k = n, t$ and $i = x, y$, and u_i^s is the i-component of the displacement vector at node s, $\mathbf{g} = (\mathrm{g}_n, \mathrm{g}_t)$ is the relative motion (gap) vector, and $\boldsymbol{f}^c$ is the contact force vector over the contact area A^c,

$$\boldsymbol{f}^c = A^c \, \boldsymbol{\sigma}^c \quad , \quad \boldsymbol{\sigma}^c = \boldsymbol{\alpha} \, \mathbf{g} = \begin{bmatrix} \alpha_n & 0 \\ 0 & \alpha_t \end{bmatrix} \begin{bmatrix} \mathrm{g}_n \\ \mathrm{g}_t \end{bmatrix} \tag{15}$$

where $\boldsymbol{\alpha}$ is the penalty term matrix, which can vary for normal and tangential gaps and even between single contact nodes. The corresponding recovered residual force is then evaluated as:

$$r_i^s = f_k^c \, \frac{\partial \mathrm{g}_k}{\partial u_i^s} \tag{16}$$

The partial derivative part of equation (16) define the direction and distribution of normal and tangential bonding forces.

The possible normal and tangential gaps for each contacting couple are evaluated by monitoring the coordinates of contacting couple nodes in each time step. Then by projecting the coordinates in the current and previous timesteps to a reference configuration, the possible gaps are calculated (Figure 5).

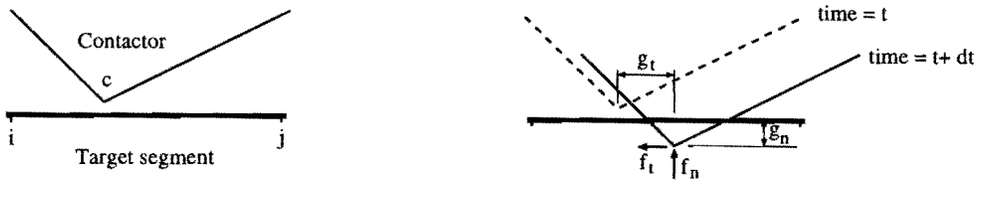

a) Before contact

b) Possible normal and tangential gaps

Figure 5: Normal and tangential gaps.

Special precautions should be taken to satisfy momentum conditions and to consider different geometry shapes of contact and target bodies (concave and convex DE boundaries). The calculated contact force has to be distributed to the target and the contactor nodes.

5 DELAMINATION INITIATION

Several criteria exist that can be used in prediction of the initiation of delamination in composite structures [7, 17]. Reasonable results can be achieved by employing maximum normal stress or strain criteria, but for obtaining more rational results, some other more sophisticated interactive criterion should be adopted. It is widely accepted that the Chang-Springer criterion can be properly used for predicting the initiation of delamination. Three dimensional representation of this criterion in local axes is defined by [12]:

$$(\frac{{\sigma_z}^2}{N^2}) + (\frac{{\sigma_{xz}}^2 + {\sigma_{yz}}^2}{T^2}) = d^2 \begin{cases} d < 1 & \text{no failure} \\ d \geq 1 & \text{failure} \end{cases} \tag{17}$$

where N and T are the unidirectional normal and tangential strengths of the bonding material, respectively.

Once the initial failure is predicted, a further criterion should be introduced to simulate the growth of the local damage as the loading continues.

6 MATERIAL MODEL

The imminence of material failure is monitored by the orthotropic Hoffman criterion [9]. According to the Hoffman criterion, a geometric yield surface is constructed from three tensile yield strengths σ_T, three compressive yield strengths σ_C, and three shear yield strengths σ_S. It may be defined as :

$$\Phi = \frac{1}{2}\boldsymbol{\sigma}^T \boldsymbol{P} \boldsymbol{\sigma} + \boldsymbol{\sigma}^T \boldsymbol{p} - \bar{\sigma}^2(\kappa) \tag{18}$$

where the projection matrix $\boldsymbol{P}$, and the projection vector $\boldsymbol{p}$ are defined based on the nine material yield strengths and a normalised yield strength $\bar{\sigma}$ (see Schellekens *et al.* [18]), and κ is a softening/hardening parameter.

The additivity postulate of computational plasticity is used to formulate the rate form of the stress return algorithm. The integration of the flow rule in a finite step is then performed by the backward Euler method coupled with the Newton-Raphson iterative scheme [1].

7 CRACK PROPAGATION

There is no immediate need for a crack propagation algorithm between discrete elements in a discontinuum mechanics scheme. Having employed a standard central difference explicit

scheme in the dynamic analysis of composites, in each time step a possible configuration is predicted from the dynamic equilibrium equations, which are formed by considering the internal forces calculated from contact/delamination interactions in the previous timestep. Therefore the current configuration offers a possible crack propagation distribution which has to be modified by the new interactions in the current timestep.

Once the delamination initiation criterion is satisfied, an interlaminar crack is formed. Forming a crack is followed by releasing energy and redistributing the forces which caused the initiation of the crack. If this procedure happens immediately after occurrence of a crack, it will lead to inappropriate energy release, and more importantly, to results that strongly depend on the size of the elements used in the analysis.

7.1 Strain softening

The main concept, borrowed from fracture mechanics, is the assumption that the fracture energy release G_f, is a material property rather than a local stress-strain curve. The implementation of the $G_f = Const.$ concept, leads to the important conclusion that the local strain-softening law depends on a fracturing zone with characteristic length, l_c, depending on the finite element mesh.

A bilinear local softening model (the Rankine softening plasticity model) is adopted in this study to account for release of energy and redistribution of forces which caused the formation of a crack. It may properly avoid the mesh dependency of the results by introducing a length scale into the softening material model [19].

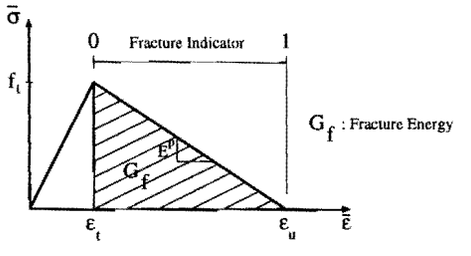

Figure 6: Fracture energy softening model.

The fracture energy release is defined as the integral of the area under the softening branch of the stress-strain curve

$$G_f = \left[\frac{1}{2} f_t \left(\epsilon_u - \epsilon_t\right)\right] l_c \tag{19}$$

where f_t is the tensile strength and ϵ_u and ϵ_t are the tensile fracture and ultimate strains respectively, and l_c is the localisation bandwidth. In general, l_c is contained within one element and in 2-D is defined based on the area of the fractured element, A, [20]

$$l_c = \sqrt{A} \tag{20}$$

The softening modulus is then defined as

$$E^p = \frac{f_t^2 \, l_c}{2G_f} \tag{21}$$

8 NUMERICAL RESULTS

8.1 Dynamic buckling analysis of a composite beam

An implicit approach combined with a fracture mechanics crack propagation algorithm was used by Grady *et al* [21], to perform a dynamic delamination buckling analysis in a composite laminate with an initial interlayer crack subjected to impact loading. The specimen geometry and impact loading are defined in Figure 7. The material properties of this clamped beamlike unidirectional $[0_n]$ graphite epoxy laminate are given in Table 8.1. Grady *et al* [21], predicted that a first mode of delamination buckling is likely to occur approximately 190 μs after the impact event begins.

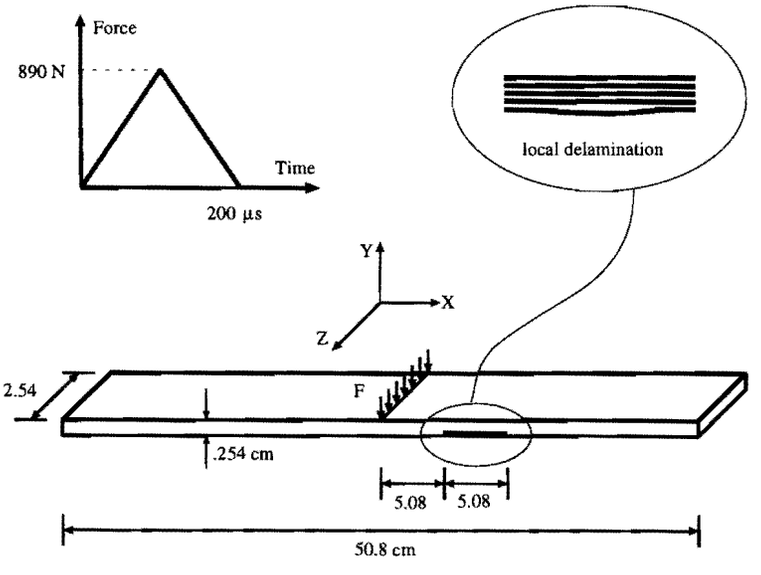

Figure 7: Specimen geometry and impact loading.

A finite element mesh with plane stress triangles (3700 nodes and 3800 elements) was used to model this problem. Four layers of discrete elements are used through the thickness. The lowest layer is predicted to experience a local delamination buckling. The critical timestep which ensures the stability of the scheme is restricted to $0.01 \mu sec.$ and as a result, $50,000$ timesteps are required for a full dynamic analysis.

The results of a linear uncracked analysis without considering delamination, and a full delamination analysis for the midpoint vertical displacements, are compared in Figure 8. It is readily concluded that the global behaviours of the beam in both cases are similar,

Table 1: Material properties for T300/1034-C graphite epoxy.

$E_{xx} = 146800MPa$	,	$G_{xx} = 6184MPa$
$E_{yy} = 11400MPa$	,	$G_{yz} = 4380MPa$
$\nu_{xy} = \nu_{yz} = 0.3$	,	$\rho = 1.55\frac{Mg}{m^3}$
$X_t = 1730MPa$	,	$X_c = 1380MPa$
$Y_t = 66.5MPa$	,	$Y_c = 26.8MPa$
$S = 133.7MPa$		

and that the local delamination buckling does not greatly affect the global response of the beam.

Figure 9 shows the time history results of vertical displacement and velocity of two adjacent nodes at the middle and at the tip of the initial crack. According to Figure 9a, delamination at the middle of the crack starts at about $t = 150\mu s$ and increases rapidly after $t = 175\mu s$, therefore the possible local buckling is predicted to occur between $t = 175\mu s$ to $t = 200\mu s$. The small difference between the two curves in this figure indicates that the crack is extended only by a small amount at the end of loading. The same conclusion may be deduced from the comparison of velocities in Figure 9.

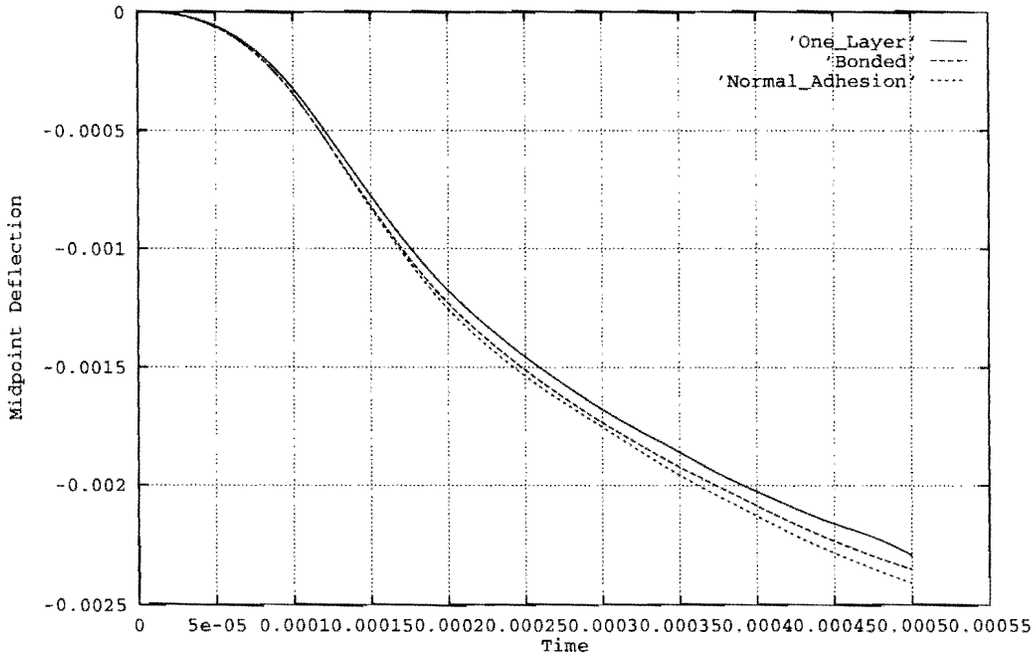

Figure 8: Midpoint Displacement

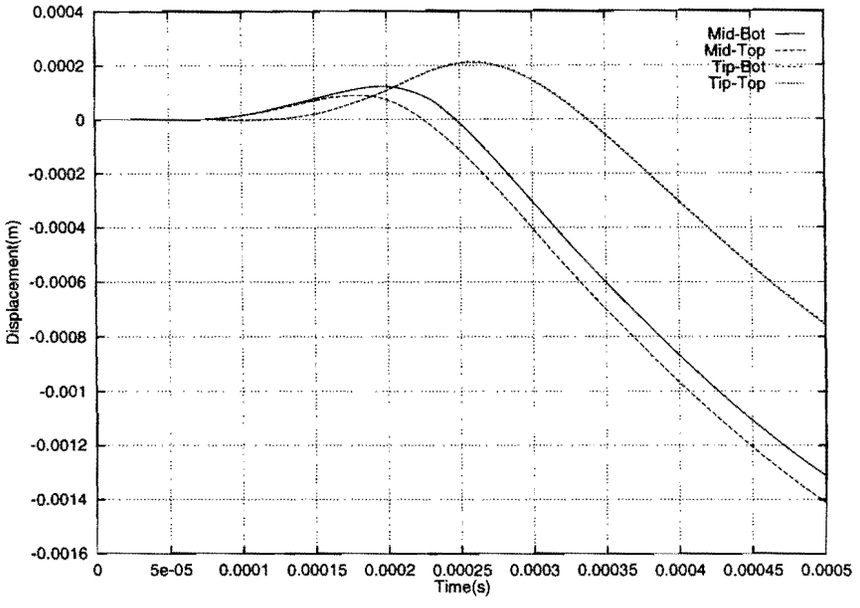

(a)Displacements.

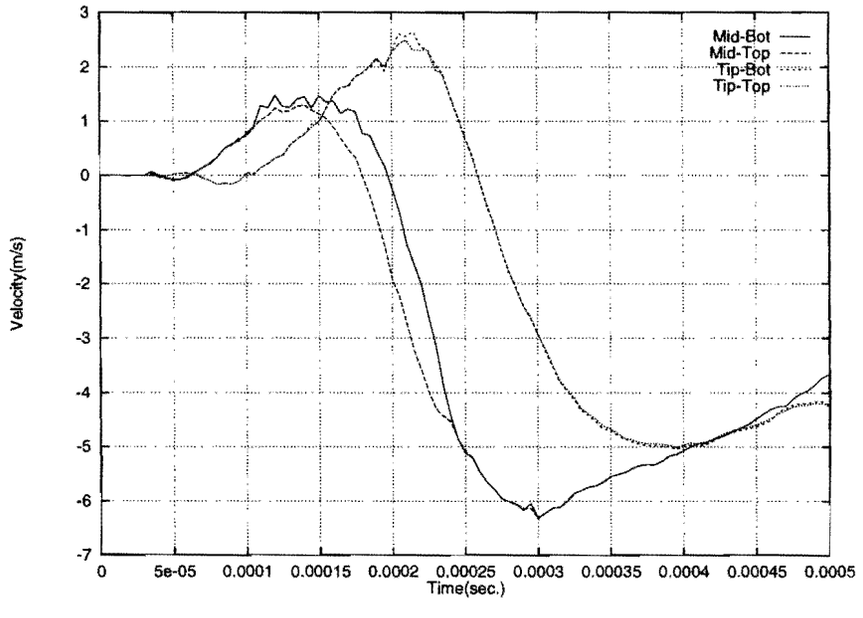

(b) Velocities.

Figure 9: Time history responses of two nodes on opposite sides of the initial crack, a)Vertical displacements, b)Vertical velocities.

8.2 Impact loading of a composite plate

A numerical simulation is undertaken to assess the performance of the method for dealing with progressive fracture and debonding phenomena in a laminated composite plate which is subjected to a high velocity impact at its centre. The impact loading is simulated by a triangular load applied from 0 to 5 μsec with a peak force of 1 kN. Because of symmetry, only one quarter of plate is modelled. Also, only the central region of this model is meshed by a DE mesh. Therefore, the possibility of fracture and delamination is only investigated in this region (See Figure 10). Material properties and other necessary information are given in Table 2 [21].

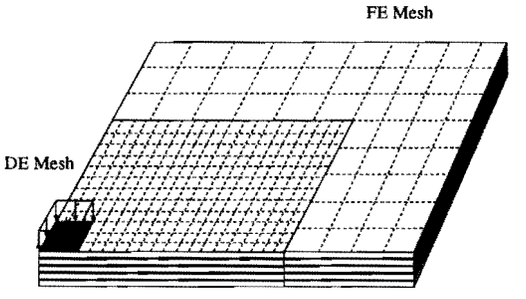

Figure 10: FE/DE mesh of the composite plate.

Table 2: Material properties for T800/P2302-19 graphite resin.

Model size $= 0.0762 \times 0.0508 \times 0.00444m$		
DE region $= 0.050 \times 0.035m$		
Ply layout $[90, 0, 90, 0, 90]$		
$E_{xx} = 152.4e3MPa$	,	$E_{yy} = 10.7e3MPa$
$\nu = 0.35$	,	$\rho = 1.55e3\frac{Kg}{m^3}$
$X_t = 2772MPa$	,	$X_c = 3100.0MPa$
$Y_t = 79.3MPa$	,	$Y_c = 231.0MPa$
$S = 132.8MPa$		

Vertical displacement responses of individual layers are shown in Figure 11. The clear discontinuities of the contours in certain parts of the model near the loading region mark the material fracture patterns. Matrix cracking has caused the cracks to be formed along the fibre direction in each layer.

Figure 12 illustrates the debonding patterns at different interfaces. It is found that the delamination patterns are mainly formed close to the material cracks. These figures depict only the DE part of the whole mesh.

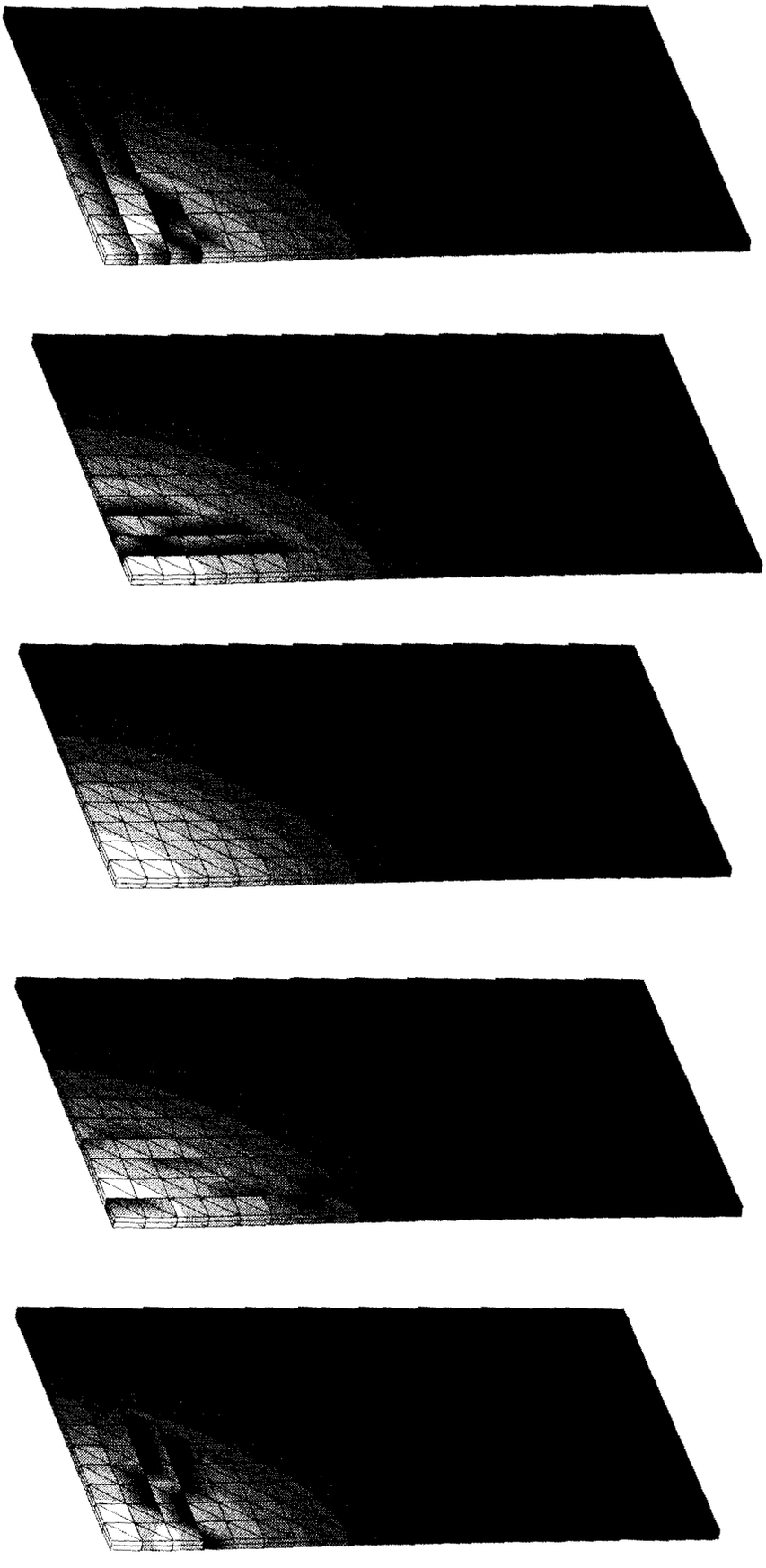

Figure 11: Vertical displacement and fracture patterns of different layers.

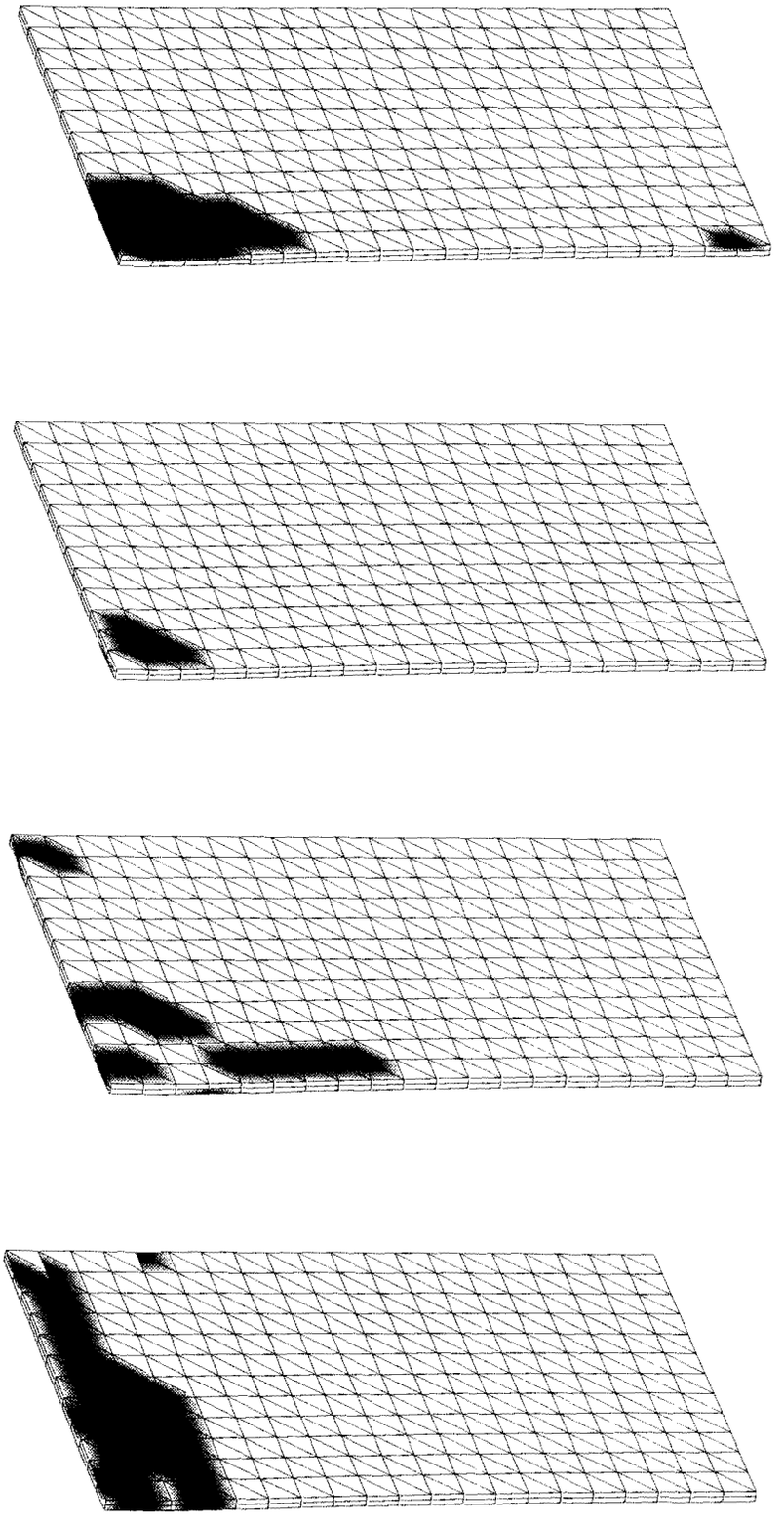

Figure 12: Delamination patterns at different interfaces of layers.

9 CONCLUSIONS

The combined finite/discrete element has proved to be an efficient algorithm for dealing with multi-fracture and fragmentation processes, which frequently arise from impact loadings on composite structures. It is also shown that the delamination behaviour in composite specimens can be effectively modelled by this method. The algorithm comprises various contact detection and contact interaction schemes to construct an efficient and reliable tool for the modelling of complex post failure phenomena. In addition to considering the potential pre-delamination contacts, it is also essential to take into account the contact and friction interactions for post debonding or fracture behaviour of composites. A major advantage of the method is that it does not require any predefined interface elements, which are considered inappropriate for efficient computational modelling of combined progressive multi-fracture and delamination analysis.

An anisotropic softening Hoffman failure criterion is adopted for specifying the initiation of a crack. A local remeshing scheme is introduced for geometric modelling of the cracks, which plays an important role in avoiding the excess distortions of the finite elements in the vicinity of cracks. The algorithm allows for both nodal separation and splitting a cracked element. The imminence of a bonding crack is predicted by the Chang-Springer criterion. A bilinear softening model is adopted for both matrix and interlaminar cracking description to prevent the mesh dependency of the results.

ACKNOWLEDGEMENTS

The third author would like to acknowledge the support received from the Ministry of Culture and Higher Education of I.R. IRAN.

References

[1] C.G. Koh, D.R.J. Owen, and D. Peric. Explicit dynamic analysis of elasto-plastic laminated composite shells: implementation of non-iterative stress update schemes for the Hoffman yield criterion. *Computational Mechanics*, **16**:307–314, 1995.

[2] P. Atherton, R. Greif, and A. Saigal. Failure analysis of P75 graphite/934 epoxy composites. In L. Cloutier and D. Rancourt, editors, *16th Canadian Congress of Applied Mechanics, CANCAM 97*, pages 51–52, 1997. Universite Laval,, Canada.

[3] S. Abrate. Impact resistance of composite materials - a review. *Applied Mechanics*, 44:155–190, 1991.

[4] B.D. Agarwal and L.J. Broutman. *Analysis and Performance of Fiber Composites.* John Wiley and Sons, inc., 1990.

[5] A.J. Kinloch, Y. Wang, J.G. Williams, and P. Yayla. The mixed-mode delamination of fiber composite materials. *Composite Science and Technology*, **47**:225–237, 1993.

[6] F.L. Matthews and R.D. Rawlings. *Composite Materials : Engineering and Science.* Chapman and Hall, 1994.

[7] S. Liu, Z.Kutlu, and F.K.Chang. Matrix cracking-induced delamination propagation in graphite/epoxy laminated composites due to a transverse concentrated load. In W.W. Stinchcomb and N.E.Ashbangh, editors, *Composite Materials : Fatigue and Fracture, ASTM STP 1156*, volume **4**, pages 86–101, 1993.

[8] A.P. Parker. *The Mechanics of Fracture and Fatigue, An Introduction.* E. & F.N. Spon Ltd., 1981.

[9] R.E. Rowlands. Strength (failure) theories and their experimental correlation. In G.C. Sih and A.M. Skudra, editors, *Handbook of Composites, Vol. 3 - Failure Mechanics of Composites*, chapter 2, pages 71–125. Elsevier Science Publishers B.V., 1985.

[10] N.J. Pagano, editor. *Interlaminar Response of Composite Materials.* Elsevier, 1989.

[11] G.E. Stavroulakis and P.D. Panagiotopoulos. On the interface debonding and frictional sliding in composites: The material inclusion problem. In W.S. Johnson, editor, *Delamination and Debonding of Materials*, pages 165–172, 1985.

[12] F.K. Chang and G.S. Springer. The strength of fiber reinforced composite bends. *Composite Materials*, **20**(1):30–45, 1986.

[13] N. Bicanic, A. Munjiza, D.R.J. Owen, and N. Petrinic. From continua to discontinua - a combined finite element / discrete element modelling in civil engineering. In B.H.V. Topping, editor, *Developments in Computational Techniques for Structural Engineering*, pages 45–58. Civil-Comp Press, 1995.

[14] A. Munjiza, D.R.J. Owen, and N. Bicanic. A combined finite-discrete element method in transient dynamics of fracturing solids. *Engineering Computations*, **12**:145–174, 1995.

[15] Y. Mi, M.A. Crisfield, and G.A.O. Davies. Failure modelling in composite structures. In M.A. Crisfield, editor, *Computational Mechanics in UK - 5th ACME Conference*, pages 36–39, April 1997. London, UK.

[16] X. Zhang, D. Hitchings, and G.A.O. Davies. Modelling composite failure and delamination during low velocity impact. In M.A. Crisfield, editor, *Computational Mechanics in UK - 5th ACME Conference*, pages 44–47, April 1997. London, UK.

[17] V. Tvergaard. Effect of fiber debonding in a whisker-reinforced metal. In *Materials Science and Engineering A : Structural Materials : Properties, Microstructure, and Processing*, volume A125(2), pages 203–213, June 1990.

[18] J.C.J. Schellekens and R. de Borst. The use of Hoffman yield criterion in finite element analyses of anisotropic composites. *Computers and Structures*, **37**(6):1087–1096, 1990.

[19] S. Mohammadi, D.R.J. Owen, and D. Peric. Delamination analysis of composites by discrete element method. In D.R.J. Owen, E. Onate, and E. Hinton, editors, *Computational Plasticity, COMPLAS V*, pages 1100–1110, March 1997. Barcelona, Spain.

[20] J.E. Grady, C.C. Chamis, and R.A. Aiello. Dynamic delamination buckling in composite laminates under impact loading : Computational simulation. In P.A. Lagace, editor, *Composite Materials: Fatigue and Fracture, ASTM STP 1012*, volume **2**, pages 137–149, 1989.

[21] M.J. Worswick, P.V. Strazincky, and O. Majeed. Dynamic fracture of fiber reinforced composite coupons. In C.T.Sun, B.V. Sankar, and Y.D.S. Rajapakse, editors, *Dynamic Response and Behaviour of Composites*, ASME AD-Vol. 46, pages 29–41, 1995.